Electrochimica Acta 55 (2010) 6058–6063

Contents lists available at ScienceDirect

Electrochimica Acta

journal homepage: www.elsevier.com/locate/electacta

The enhancing power of iodide on corrosion prevention of mild steel in the presence of a synthetic-soluble Schiff-base: Electrochemical and surface analyses

Mohsen Lashgari [a,*], Mohammad-Reza Arshadi [b], Somaieh Miandari [a]

[a] Department of Chemistry, Institute for Advanced Studies in Basic Sciences (IASBS), Gava-Zang Blvd., Zanjan 45137-66731, Iran
[b] Department of Chemistry, Sharif University of Technology, PO Box 11365-9516, Tehran, Iran

ARTICLE INFO

Article history:
Received 14 February 2010
Received in revised form 19 May 2010
Accepted 20 May 2010
Available online 27 May 2010

Keywords:
Mild steel corrosion
Schiff-base ligand
Desorption–adsorption process
Inhibitors *in vacuo*
Inhibition mechanism

ABSTRACT

The inhibitory action of N,N′-1,3-propylen-bis(3-methoxysalicylidenimine) {PMSI} on mild steel corrosion in sulfuric acid medium was investigated through electrochemical methods and evaluations based on infrared spectroscopy and scanning electron micrographs. The studies revealed that the molecule is a good mixed-type inhibitor (mostly anodic), acts as a multi-dentate ligand and repels the corrosive agents by hydrophobic forces. Its adsorption on metal surface has a physicochemical nature and obeys the Langmuir isotherm. At a critical (optimum) concentration, an anomalous inhibitory behavior was observed and interpreted at microscopic level by means of desorption/adsorption process and *horizontal* ↔ *vertical* hypothesis. The addition of iodide into acid moreover causes a synergistic influence, a substantial enhancement on inhibitory performance. Finally, using isolated inhibitor calculations at B3LYP/6-31G + (d,p) level of theory, the equilibrium geometry of PMSI was determined and the energy required for hindrance avoidance was predicted.

1. Introduction

Due to its high mechanical properties and low cost [1], mild steel has a wide application in various industries as construction material for chemical reactors, heat exchange and boiler systems, storage tanks, and oil and gas transport pipelines.

Protection of the equipments and vessels against corrosion is one of chief concerns of the maintenance and design engineers. The use of corrosion inhibitors, whenever possible, is one of the most effective methods for this concern [2]. The materials used as corrosion inhibitors are chemicals, organic or inorganic, which when added in small quantities to the corrosive environment, reduce the deterioration of metals. The mechanism of this protection depends on the metal and inhibitor under consideration. In most cases, however, it is due to the adsorption of these compounds on the surface of metals which can reduce the extent of corrosion through thermodynamics or kinetics phenomena [3].

Schiff-bases are among azomethine compounds [4,5] that have recently attracted more attentions in the field of corrosion inhibition science [6–11]. The reason is mainly due to the ease of synthesis from relatively inexpensive starting-materials and their eco-friendly properties, harmless for environment [12]. In addition, the inhibitory performance of these compounds is predicted to be high because of various adsorbing centers available in the molecule. The efficiency of the molecule can further be enhanced through a synergistic effect, resulting from specific adsorption of a non-corrosive anion like as iodide which can be bridged between the inhibitor cation and the positively charged surface in acid solutions [13,14].

Besides the factors mentioned above, an industrially suitable inhibitor should be soluble in aqueous environments, e.g. in acid washing systems. The molecule synthesized and examined here (PMSI; Fig. 1), fortunately, has this property. The objective of this work is to provide a mechanistic understanding of the phenomenon of mild steel corrosion in sulfuric acid medium in the presence of PMSI inhibitor. We moreover demonstrate the power of iodide (in small quantity; 10^{-3} M), on corrosion prevention of mild steel in the presence of the synthetic Schiff-base.

2. Experimental

2.1. Materials and solutions

A 2:1 molar ratio mixture of 2-hydroxyl-3-methoxy-benzaldehyde and 1,3-propandiamine was dissolved in ethanol, heated and refluxed for about an hour. The condensate was then cooled and filtered. The filtrate was characterized by NMR (nuclear magnetic resonance), FT-IR (Fourier transform infrared) and UV–vis (ultraviolet–visible) spectra. All chemicals used were analytical grade reagents obtained from Merck Chemical Com-

* Corresponding author. Tel.: +98 241 4153205; fax: +98 241 4153232.
E-mail address: Lashgari@iasbs.ac.ir (M. Lashgari).

0013-4686/$ – see front matter © 2010 Elsevier Ltd. All rights reserved.
doi:10.1016/j.electacta.2010.05.066

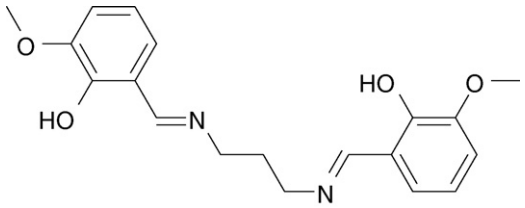

Fig. 1. Structural formula of N,N′-1,3-propylen-bis(3-methoxysalicylidenimine) {PMSI} Schiff-base.

pany. The steel specimen with the following composition (wt.%; determined by quantometric analysis): 0.021% Cr, 0.0033% Ni, 0.035% Al, 0.130% C, 0.546% Mn and the remainder iron, was used. The aggressive solution was made by AnalaR grade sulfuric acid and double-distilled water. The concentration of acid solution was 0.5 M and those of inhibitor were $C_{inhib} \leq 0.01$ M. For the synergistic experiments, KI concentration was 0.001 M.

2.2. Electrochemical studies

The mild steel embedded in epoxy resin with exposed area of 0.5 cm^2 was used as working electrode. Before each experiment, the working surface was ground with successive SiC abrasive papers up to 1200 grit, degreased by acetone and washed with distilled water and ethanol then dried in air [15].

The auxiliary electrode was a platinum foil and the reference was Ag/AgCl (3 M KCl) electrode coupled to a Luggin capillary with the tip placed approximately 1 mm from the working surface. The reaction vessel was a three-electrode chamber connected to an AUTOLAB/PGSTAT30 instrument. The experimental data of Tafel polarization curves and electrochemical impedance spectra (EIS) were processed by GPES and FRA (4.9) softwares, respectively. In polarization measurement, the working electrode was immersed in the test solution at open circuit potential (OCP) for the time needed to achieve a steady state potential. Then the potential of working electrode was scanned at a rate of 1 mV/s, from cathodic to anodic direction.

The percent inhibition efficiency, IE (%), of PMSI was calculated from the following equation [16]:

$$\text{IE}\ (\%) = \left(1 - \frac{i'_{corr}}{i_{corr}}\right) \times 100 \quad (1)$$

where i_{corr} and i'_{corr} are corrosion current densities measured in the absence and presence of the inhibitor, respectively.

Impedance measurements were carried out at OCP. After immersion of the specimen in the test solution, prior to each measurement, a stabilization period of 15 min was observed which proved sufficient to attain a stable value. A sinusoidal potential with amplitude of 10 mV (rms), superimposed on OCP, was applied. The frequency of this ac signal was scanned from 100 kHz to 10 mHz. All EIS measurements were performed at room temperature. The inhibition efficiency for this method was calculated from this equation [16]:

$$\text{IE}\ (\%) = \left(\frac{R_{ct} - R^o_{ct}}{R_{ct}}\right) \times 100 \quad (2)$$

where R^o_{ct} and R_{ct} are charge transfer resistance in the absence and presence of the inhibitor, respectively. All experiments were performed twice and the mean results were reported.

2.3. Surface analysis

The mild steel specimens used here (10 mm × 10 mm) were prepared in the same manner explained above for electrochemical studies. They were immersed in the respective corrosive solution for 24 h [17]. Then the specimens were washed with distilled water and ethanol, dried and stored in a moisture-free desiccator. The surface morphology was studied *ex situ* by a SEM VEGA© TESCAN microscope. Infrared spectra of the inhibitor film on metal surface were also obtained by a Thermo Nicolet NEXUS™ 670 FT-IR spectrometer.

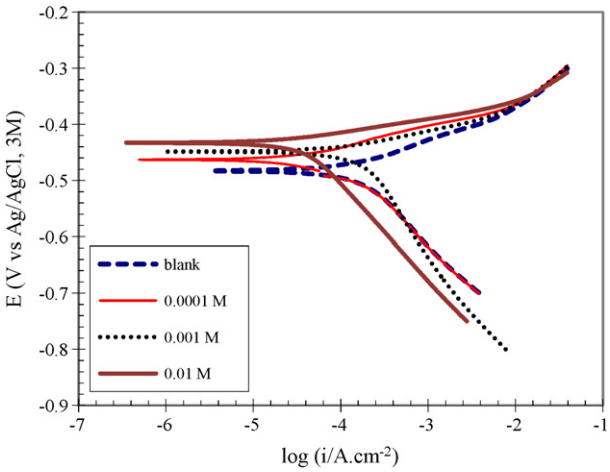

Fig. 2. Polarization curves for mild steel corrosion in 0.5 M H_2SO_4 solution in the presence of PMSI at various inhibitor concentrations.

2.4. Isolated inhibitor calculations

Without going to the details of computational strategies and quantum electrochemical models developed recently in the field of corrosion inhibition science [18–20], here, we simply carried out some quantum chemical calculations on the inhibitor molecule *in vacuo* using density functional theory (DFT; B3LYP version [21]) and applying a relatively large standard 6-31G + (d,p) basis set. The calculations were performed on a PC (3 GHz) via *Gaussian 03* suit of computer codes [22].

3. Results and discussion

3.1. Electrochemical measurements

The polarization curves of mild steel in sulfuric acid medium, in the presence and absence of the inhibitor compound, are presented in Fig. 2 and quantified in Table 1. As it can be seen here, the presence of molecule in acid solution affects on both polarization branches, which causes the corrosion potential (E_{corr}) being more positive at all inhibitor concentrations as compared with that of blank solution. This means that the molecule under consideration acts as a mixed-type inhibitor (mostly anodic; $E^{inhib}_{corr} > E^{blank}_{corr}$).

Data presented in Table 1 also indicate a decrease occurring in corrosion current density (i_{corr}) as the inhibitor concentration increases. This trend continues up to an optimum concentration of 0.005 M. Beyond that the favorable effect will turn suddenly to an unfavorable one. The distinguished behavior witnessed for this critical concentration is evidently reconfirmed by impedance measurements as depicted in Fig. 3; at this concentration, the diameter of semi-circle becomes surprisingly large. To justify this anomalous behavior, it should be noticed that by increasing the inhibitor concentration, the molecules are generally reoriented from horizontal to vertical mode of adsorption due to area releasing effect and ensemble energy minimization [23]; the horizontal is predominant at low surface coverages but it changes to the vertical as the concentration increases. At the critical-optimum concentration,

Table 1
Potentio-dynamic results of the mild steel corrosion in 0.5 M H_2SO_4 medium (purged by nitrogen) containing PMSI inhibitor.

C_{PMSI} (M)	i_{corr} (μA/cm²)	$-\beta_c$ (mV/dec)	β_a (mV/dec)	R_p (Ω cm²)	$-E_{corr}^{obs}$ [a] (mV $_{Ag/AgCl,3M}$)	$-E_{corr}^{calc}$ [b] (mV$_{Ag/AgCl,3M}$)	IE (%)
Blank	298.80	68	174	28.65	483	488	–
5×10^{-5}	99.40	28	182	39.34	453	441	66.73
10^{-4}	80.90	32	152	46.00	463	445	72.93
5×10^{-4}	78.13	35	153	53.87	460	441	73.85
10^{-3}	70.31	25	169	46.09	445	432	76.47
5×10^{-3}	54.35	27	164	64.05	445	433	81.81
10^{-2}	60.81	24	172	53.12	433	426	79.65

[a] Breaking point of the polarization curves where the current direction is reversed.
[b] Calculated from extrapolation of Tafel (anodic and cathodic) lines.

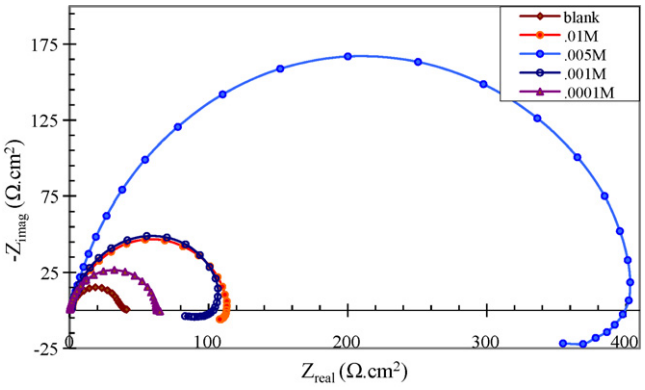

Fig. 3. Impedance plots of mild steel in 0.5 M H_2SO_4 in the presence of PMSI inhibitor at various concentrations.

where both forms (horizontal and vertical) are counterbalance, an infinitesimal decreasing in surface coverage causes the vertical mode of adsorption to be completely reverted. The decrease is taken place instantaneously through accumulative desorption of the inhibitor molecules adsorbed vertically. The possibility of accumulative desorption resulting from lateral interactions [24], moreover provides a reason why the inhibitor efficiency does not increase above the optimum.

At the balance (optimum), the instantaneous desorption process mentioned above is dynamically reversible and synchronized with the inhibitor adsorption on unoccupied (previously released) sites. This simultaneous desorption/adsorption process seems to be responsible for anomalous behavior of the inhibitor molecules at the critical (optimum) concentration. By accepting this hypothesis, i.e. the synchronized desorption ↔ adsorption process, we have therefore to observe an inductive loop in impedance spectra at low frequencies [3], as seen in Fig. 3. This indirectly justifies why the interesting-inductive loop does not appear below the optimum; explanatorily, there is no inductive loop since there is no alternation on the mode of adsorption (the parallel exists only and no desorption is taken place!).

By applying the following relation [16], the surface coverage (θ) was calculated.

$$\theta = \frac{(i_{corr} - i'_{corr})}{i_{corr}} \quad (3)$$

To determine the adsorption behavior of the molecule under consideration, we applied various linearized isotherms [25,26]. The best correlation was obtained through Langmuir model with the regression coefficient, R^2 equal to 0.9998 (see Fig. 4). Using the Langmuir relation, Eq. (4), the value of adsorption equilibrium constant (K_{ads}) was calculated.

$$\frac{C_{inhib}}{\theta} = C_{inhib} + \frac{1}{K_{ads}} \quad (4)$$

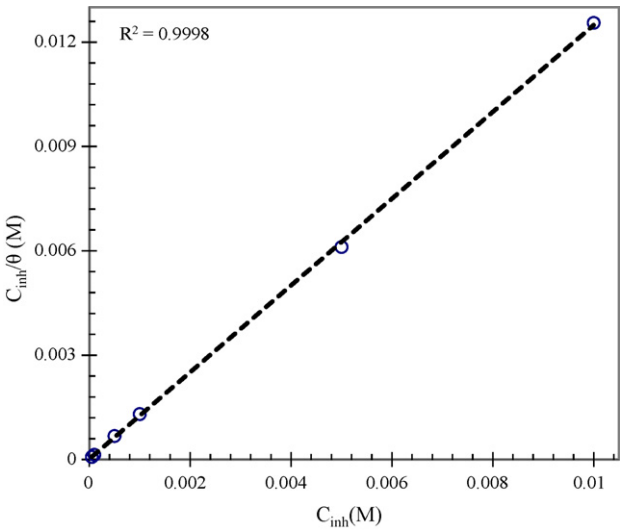

Fig. 4. Langmuir isotherm for the adsorption of PMSI on mild steel surface in 0.5 M H_2SO_4, determined from polarization data.

K_{ads} was found to be 5000 and the corresponding standard free energy, ΔG^o_{ads} was calculated to be −36.8 kJ/mol. The latter is close to −40 kJ/mol and indicates a relatively strong inhibitor adsorption [27,28].

The effect of iodide ions on the corrosion rate and inhibition efficiencies was also studied through impedance measurements. The results are summarized in Table 2 and the impedance plots are included in Fig. 5. Concerning this part of study, there are several points worthy of considerations:

1. Addition of 10^{-3} M potassium iodide alone to the acid solution increased the charge transfer resistance, R_{ct}, considerably and resulted in a percent inhibition efficiency of 64%. This indicates

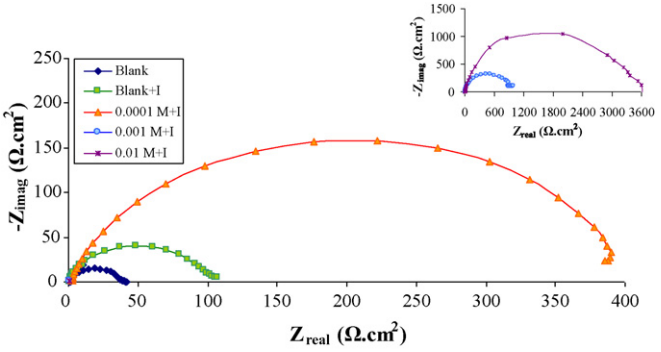

Fig. 5. Impedance plots of mild steel in 0.5 M H_2SO_4 in the presence of iodide (10^{-3}M) and PMSI at various inhibitor concentrations.

Table 2
Electrochemical impedance parameters for mild steel corrosion in 0.5 M H_2SO_4 medium (purged by nitrogen) in the presence of PMSI inhibitor.

C_{PMSI} (M)	$-E_{ocp}$ ($mV_{Ag/AgCl,\ 3M}$)	R_s ($\Omega\,cm^2$)	R_{ct} ($\Omega\,cm^2$)	C_{PE} ($\mu F\,cm^{-2}$)	n	IE (%)	S
Blank	466[a]	1.078	36.07	69.20	0.889	–	–
	472[b]	0.923	100.89	73.20	0.855	64.24	
10^{-4}	470[a]	0.267	64.00	59.75	0.905	43.64	2.21
	446[b]	2.082	396.00	26.97	0.857	90.89	
10^{-3}	457[a]	1.076	112.20	81.05	0.866	67.84	3.14
	448[b]	1.925	988.00	30.50	0.830	96.34	
10^{-2}	452[a]	1.447	115.70	68.72	0.855	68.82	10.23
	404[b]	0.269	3300.00	15.52	0.921	98.91	

[a] Determined in the absence of iodide ions (10^{-3} M).
[b] Determined in the presence of iodide ions (10^{-3} M).

that the iodide ions can be considered as an inhibitor for mild steel/H_2SO_4 system.
2. The addition of iodide into the inhibitor-acid solution, improved the inhibition efficiencies considerably, over 98% for 10^{-2} M PMSI.
3. A non-ideal capacitive behavior is clearly observed in Fig. 5, as occurrence of a depressed semi-circle. This behavior is normally observed in most EIS studies of the corrosion inhibitor systems and it is attributed to the surface roughness of the metal. For this reason, the double layer capacitance, C_{dl}, has been replaced with the constant phase element, C_{PE}. The latter quantity is calculated by the following equation as explained elsewhere [16]:

$$C_{PE} = \frac{Y\omega^{n-1}}{\sin(n\pi/2)} \quad (5)$$

where ω is the angular frequency for which the imaginary part of impedance is maximum. Y and n are two frequency independent parameters. The values of C_{PE} as well as the surface roughness, n, are given in Table 2.

Included in Table 2 are also the values of S, synergism parameter calculated by this relation [13,28]:

$$S = \frac{1 - \eta_I - \eta_{PMSI} + \eta_I\eta_{PMSI}}{1 - \eta_{I.PMSI}} \quad (6)$$

where η_I and η_{PMSI} are the inhibition efficiencies of iodide and PMSI, respectively, and $\eta_{I.PMSI}$ is that of mixture. From the values of S (all over one) we can conclude that the synergism occurred in all the trials and no antagonism was observed [13,28].

3.2. Surface analysis studies

Fig. 6 represents the SEM images of mild steel samples under various conditions studied in this work. Fig. 6(A) is the image of

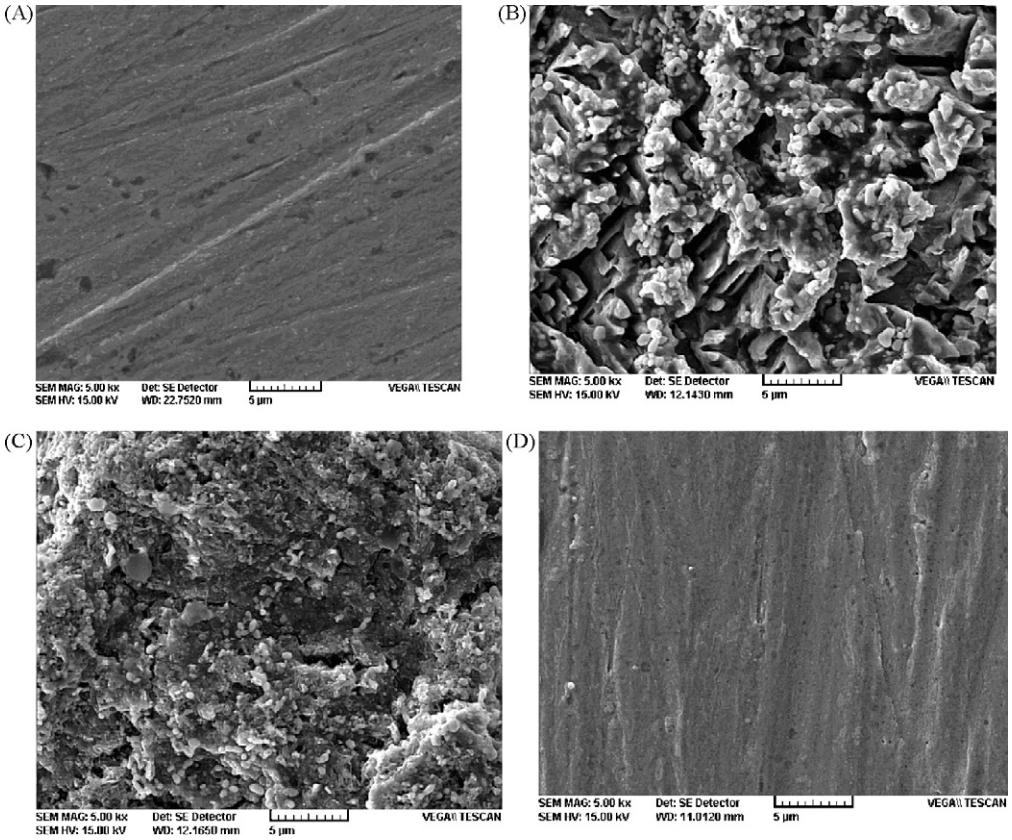

Fig. 6. SEM micrographs of mild steel before (A) and after immersion in 0.5 M H_2SO_4 for 24 h, in the absence (B) and presence (C) of 0.01 M PMSI, containing (D) 0.001 M potassium iodide.

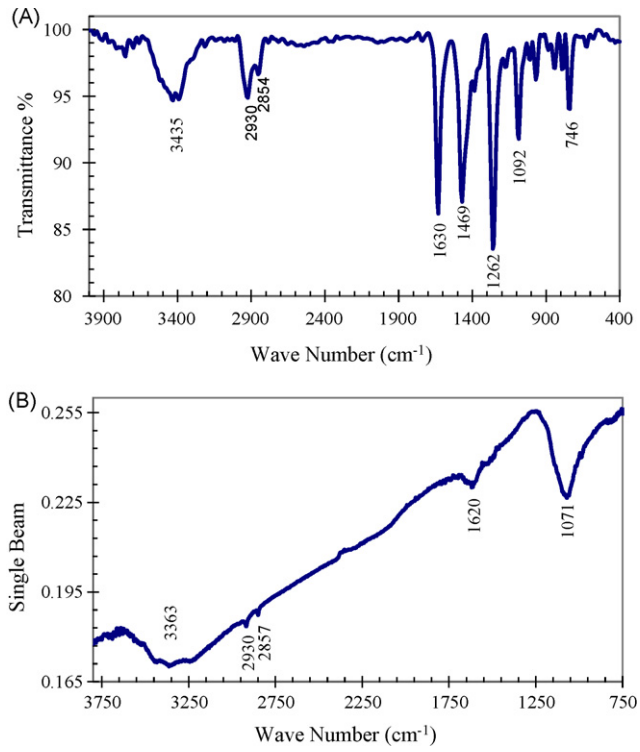

Fig. 7. FT-IR spectra of PMSI inhibitor: (A) in KBr matrix and (B) on metal surface, measured after 24 h immersion of the specimen in the acid solution containing 0.01 M PMSI and 0.001 M KI.

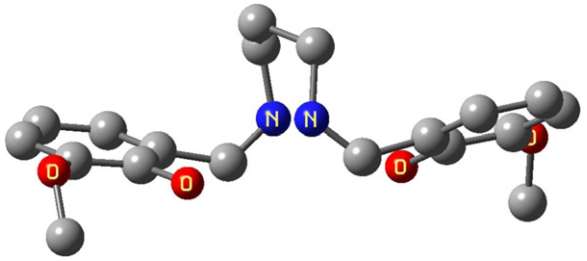

Fig. 8. The equilibrium structure of the Schiff-base, optimized *in vacuo* at B3LYP/6-31 + G(d,p) level of theory.

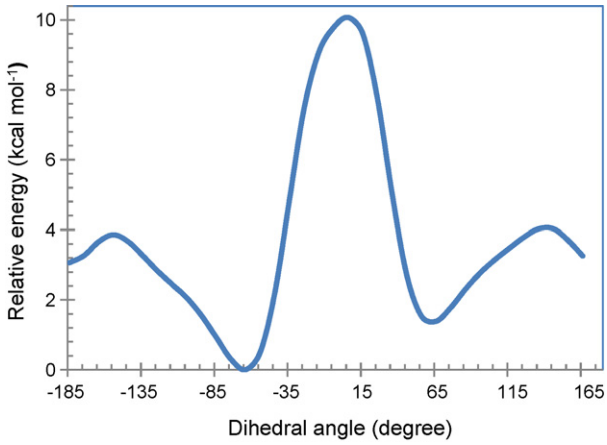

Fig. 9. Energy variation with methyl rotation around C-O bond, calculated via B3LYP/6-31G + (d,p) method.

newly polished sample before placing in acid solution. Fig. 6(B) shows the same sample after immersing in the blank solution for 24 h. The appearance of corrosion products is clearly observed. Fig. 6(C) was taken from a sample in acid solution containing PMSI alone and finally Fig. 6(D) represents the metal sample after immersing in solution containing both PMSI (10^{-2} M) and potassium iodide (10^{-3} M). The resemblance of the Fig. 6(D) to that of (A) is appreciable and proves the excellent corrosion prevention of PMSI and iodide ions combined. For this combination, moreover, a study of reflective FT-IR was performed on the adsorbed inhibitor film. The results are shown in Fig. 7.

Fig. 7(A) was taken from PMSI in KBr matrix and Fig. 7(B) from the film on metal surface after immersion of the sample in the acid solution containing 0.01 M PMSI and 0.001 M KI. Table 3 compares the IR frequencies, between the transmissive and reflective spectra. From Fig. 7 and Table 3, we observe a broadening effect and shift in the frequencies of the adsorbing functional groups. Data tabulated here also indicate that there is no interaction between the aliphatic moieties and metal surface.

3.3. Theoretical calculations and inhibition mechanism

Fig. 8 illustrates the equilibrium geometry of PMSI optimized *in vacuo*. This figure demonstrates that the zigzag shape of the propylene chain sketching within structural formula (Fig. 1) is not thermodynamically stable and deforms to a handle shape as shown in Fig. 8. The shrinkage of the aliphatic chain permits both nitrogen atoms coming close and the distance between them decreases to the value of 2.88 Å. Furthermore, the figure represents a non-zero dihedral angle between methoxy and aromatic ring; the torsion angle is about −64°. On the basis of geometrical data depicted here, one may conclude that the methyl group has a hindrance effect on inhibitor adsorption through aromatic rings and heteroatom centers, while the empirical data do not support this conclusion. This is possibly because of hindrance avoidance occurring through internal rotation of the methyl around C–O bond. Fig. 9 represents the energy changes during this rotation. The figure also illustrates two more stable minima. The first is a global minimum, standing for the structure optimized without any restriction. While, the second is slightly unstable (+1.387 kcal/mol) and corresponds with a hindering-free geometry with dihedral angle of +66° at which the methyl group is being upwards. The destabilization energy seems to be provided by molecules thermal motions with heat releasing through strong metal/inhibitor interactions. For this transformed structure, i.e. the geometry favored for adsorption through aromatic rings and heteroatom centers, the lack of interaction between aliphatic moieties and metal surface is also approved by experimental data; no shift observed in IR frequencies of the aliphatic moieties (see Table 3). It alternatively indicates that during the

Table 3
FT-IR results of PMSI inhibitor; see Fig. 7.

Reflective FT-IR frequencies (cm^{-1})	FT-IR frequencies (cm^{-1})	Functional groups
3363 (broad)	3435	OH of phenol
2930, 2857	2930, 2854	C–H (aliphatic and aromatic)
1620	1630	C=N
1250–1520 (broad)	1469	C=C
1250–1520 (broad)	1262	C–O

inhibitor adsorption, the moieties (methyl and propylene) are most probably pushed away. This orientation of the aliphatic groups deems to have a positive effect on the inhibitory action by repelling the aqueous corrosive agents by hydrophobic forces [29].

4. Conclusion

1. The aqueous soluble Schiff-base investigated here (PMSI) is among easily synthesized eco-friendly compounds, behaves as a mixed-type (mostly anodic) inhibitor for mild steel corrosion in sulfuric acid medium. Its inhibitory action enhances with increasing the inhibitor concentration up to an optimum value of 0.005 M. At this concentration, a dynamic desorption/adsorption process is responsible for distinct behavior of the molecule at metal/solution interface.
2. An excellent inhibition power is witnessed for the mixture of PMSI and iodide ions, while the iodide by itself shows a relatively good inhibitive performance.
3. PMSI adsorbs on metal surface via aromatic rings, imine groups (C═N) and oxygen centers whereas the aliphatic moieties are pushed away, towards the solution and repel the aqueous aggressive species by hydrophobic forces.
4. The adsorption process of PMSI follows the Langmuir isotherm model.

Acknowledgement

The authors would like to acknowledge the financial support of the research council of this institute (G2009IASBS124).

References

[1] Z. Tao, S. Zhang, W. Li, B. Hou, Corros. Sci. 51 (2009) 2588.
[2] R.W. Revie, H.H. Uhlig, Corrosion and Corrosion Control, John Wiley and Sons, New York, 2008 (Chapter 17).
[3] V.S. Sastri, Corrosion Inhibitors: Principle and Applications, John Wiley and Sons, New York, 1998, pp. 51–159, 280.
[4] R.N. Butler, F.L. Scott, T.A.F. O'Mahony, Chem. Rev. 73 (1973) 93.
[5] N.E. Borisova, M.D. Reshetova, Y.A. Ustynyuk, Chem. Rev. 107 (2007) 46.
[6] K.S. Jacob, G. Parameswaran, Corros. Sci. 52 (2010) 224.
[7] E. Naderi, M. Ehteshamzadeh, A.H. Jafari, M.G. Hosseini, Mater. Chem. Phys. 120 (2010) 134.
[8] I. Ahamad, R. Prasad, M.A. Quraishi, Corros. Sci. 52 (2010) 933.
[9] A.M. Abdel-Gaber, M.S. Masoud, E.A. Khalil, E.E. Shehata, Corros. Sci. 51 (2009) 3021.
[10] H. Keleş, M. Keleş, İ. Dehri, O. Serindağ, Mater. Chem. Phys. 112 (2008) 173.
[11] R.A. Prabhu, T.V. Venkatesha, A.V. Shanbhag, G.M. Kulkarni, R.G. Kalkhambkar, Corros. Sci. 50 (2008) 3356.
[12] C. Küstü, K.C. Emregül, O. Atakol, Corros. Sci. 49 (2007) 2800.
[13] E. Kálmán, I. Felhősi, F.H. Kármán, I. Lukovits, J. Telegdi, G. Pálinkás, in: M. Schütze (Ed.), Corrosion and Environmental Degradation, vol. 1, Wiley-VCH, Weinheim, Germany, 2000 (Series of Materials Science and Technology. A Comprehensive Treatment, Chapter 9).
[14] F. Bentiss, M. Lebrini, M. Traisnel, M. Lagrenée, J. Appl. Electrochem. 39 (2009) 1399.
[15] K. Tebbji, I. Bouabdellah, A. Aouniti, B. Hammouti, H. Oudda, M. Benkaddour, A. Ramdani, Mater. Lett. 61 (2007) 799.
[16] M.G. Hosseini, S.F.L. Mertens, M. Ghorbani, M.R. Arshadi, Mater. Chem. Phys. 78 (2003) 800.
[17] E. Bayol, T. Gürten, A.A. Gürten, M. Erbil, Mater. Chem. Phys. 112 (2008) 624.
[18] M. Lashgari, M.R. Arshadi, M. Biglar, Chem. Eng. Commun. 197 (2010) 1303.
[19] M. Lashgari, M.R. Arshadi, V.S. Sastri, J. Electrochem. Soc. 154 (2007) P93.
[20] M. Lashgari, M.R. Arshadi, Gh.A. Parsafar, V.S. Sastri, Corrosion (Houston) 62 (2006) 199.
[21] M. Lashkari, M.R. Arshadi, Chem. Phys. 299 (2004) 131.
[22] M.J. Frisch, G.W. Trucks, H.B. Schlegel, G.E. Scuseria, M.A. Robb, J.R. Cheeseman, J.A. Montgomery Jr., T. Vreven, K.N. Kudin, J.C. Burant, J.M. Millam, S.S. Iyengar, J. Tomasi, V. Barone, B. Mennucci, M. Cossi, G. Scalmani, N. Rega, G.A. Petersson, H. Nakatsuji, M. Hada, M. Ehara, K. Toyota, R. Fukuda, J. Hasegawa, M. Ishida, T. Nakajima, Y. Honda, O. Kitao, H. Nakai, M. Klene, X. Li, J.E. Knox, H.P. Hratchian, J.B. Cross, C. Adamo, J. Jaramillo, R. Gomperts, R.E. Stratmann, O. Yazyev, A.J. Austin, R. Cammi, C. Pomelli, J.W. Ochterski, P.Y. Ayala, K. Morokuma, G.A. Voth, P. Salvador, J.J. Dannenberg, V.G. Zakrzewski, S. Dapprich, A.D. Daniels, M.C. Strain, O. Farkas, D.K. Malick, A.D. Rabuck, K. Raghavachari, J.B. Foresman, J.V. Ortiz, Q. Cui, A.G. Baboul, S. Clifford, J. Cioslowski, B.B. Stefanov, G. Liu, A. Liashenko, P. Piskorz, I. Komaromi, R.L. Martin, D.J. Fox, T. Keith, M.A. Al-Laham, C.Y. Peng, A. Nanayakkara, M. Challacombe, P.M.W. Gill, B. Johnson, W. Chen, M.W. Wong, C. Gonzalez, J.A. Pople, Gaussian 03, Revision B. 03, Gaussian, Inc., Pittsburgh PA, 2003.
[23] M. Lashgari, M.R. Arshadi, Gh.A. Parsafar, Corrosion (Houston) 61 (2005) 778.
[24] K. Babić-Samardžija, L. Corina, N. Hackerman, A.R. Barron, A. Luttge, Langmuir 21 (2005) 12187.
[25] S. Miandari, Inhibitory behavior of some synthetic Schiff base compounds as corrosion inhibitors of mild steel in acidic media, M.Sc. thesis, Zanjan university, Zanjan, Iran, 2009, p. 66.
[26] J.M. Bastidas, P. Pinilla, E. Cano, J.L. Polo, S. Miguel, Corros. Sci. 45 (2003) 427.
[27] M.G. Hosseini, S.F.l. Mertens, M.R. Arshadi, Corros. Sci. 45 (2003) 1473.
[28] L. Valek, S. Martinez, Mater. Lett. 61 (2007) 148.
[29] G. Gao, C.H. Liang, H. Wang, Corros. Sci. 40 (2007) 1833.